International Journal of Thin Films Science and Technology

http://dx.doi.org/10.18576/ijtfst/140305

Deposition Temperature Effects on Structural and Optical Properties of RF-Sputtered Tungsten Disulfide Thin Films

A. A. Alahmari[1,2,*], *El Sayed Yousef*[1,2] *and H. H. Hegazy*[1,2]

[1]Central Labs, King Khalid University, AlQura'a, Abha, P.O. Box 960, Saudi Arabia
[2]Department of Physics, Faculty of Science, King Khalid University, P.O. Box 9004, Abha, Saudi Arabia

Received: 2 Mar. 2025, Revised: 12 Jun. 2025, Accepted: 22 Jul. 2025
Published online: 1 Sep. 2025

Abstract: Tungsten disulfide (WS_2) thin films were deposited using RF sputtering. The study investigated the impact of substrate temperature, ranging from room temperature to 400 °C, on the structural and optical properties. Structural characterization using XRD, Raman spectroscopy, SEM, and AFM reveals that thin films deposited between 200 °C and 400 °C are polycrystalline. All films showed high optical transmittance (>80%) in the visible spectrum. The optical energy gap for films prepared at room temperature was determined to be 2.46 eV and decreased to 1.79 eV with increasing substrate temperature. Notably, thin films deposited at 400 °C exhibited slightly wider band gaps, which may be attributed to non-stoichiometric WS_{2-x} as confirmed via EDX. This study illustrates that WS_2 thin films have structural and optical characteristics that render them viable candidates for use as window layers in thin-film solar cell devices, providing a basis for further development and integration in photovoltaic technologies.

Keywords: WS_2 thin films, RF sputtering, substrate temperature, Band gap energy, refractive index, Raman spectra, AFM.

1 Introduction

Transition metal dichalcogenides (TMDs), with their distinctive layered structure and configurable bandgap, are a promising material for next-generation electrical and optoelectronic applications [1]. TMDC bandgaps have a size impact and change from indirect to direct in the monolayer [2]. As an example, when MoS_2 is formed into a single layer, its direct bandgap of 1.8 eV becomes significantly larger than its bulk indirect bandgap of 1.3 eV. Graphene and TMDCs, as 2D materials, exhibit a wide variety of intriguing layer-dependent characteristics that deviate substantially from those of the bulk materials. Tungsten disulfide (WS_2) is a well-known transition metal dichalcogenide (TMD) with unique properties. Its excellent stability at high temperatures, with low oxidation seen up to 300 °C, makes it appropriate for various applications [3]. This behavior allows versatile applications such as solar cells, photodetectors, transistors, and electroluminescent devices [4]. RF magnetron sputtering is a widely used method for depositing WS_2 thin films, owing to its scalability, repeatability, and precise control over deposition conditions [5]. The substrate temperature significantly influences nucleation, crystallinity, and stoichiometry during thin-film growth. Increased temperatures enhance adatom mobility, resulting in enhanced crystal growth. Nonetheless, excessively elevated temperatures may induce defects or phase transitions. Understanding how substrate temperature affects the structural and optical properties of WS_2 is critical for improving performance in practical applications.

Despite growing interest in WS_2 thin films for optoelectronic and photovoltaic applications, not much is known about how the temperature of the substrate affects the film structure and optical properties. There has not been enough research on how changes in substrate temperature during RF sputtering affect band gap energy, optical transmittance, morphology, and crystallinity. In this study, we investigated systematically how substrate temperature affects the structural and optical properties of WS_2 thin films produced using RF sputtering. Our findings offer helpful recommendations for optimizing the growth conditions of WS_2 thin films.

2 Experimental Details

2.1. Preparation of WS_2 thin films

Thin films of WS_2 were deposited by HHV ATS 500 RF sputtering coater at different substrate temperatures. Cleaning the substrates is a crucial step performed just before thin film deposition to ensure strong adhesion. Soda-lime glass substrates were cleaned using a detailed multi-step process to ensure proper film adhesion. This included chemical cleaning with Decon 90, acetone, methanol, nitric acid, and repeated rinsing in deionized water. Further cleaning involved ultrasonic treatment in isopropyl alcohol and deionized water (DIW) for approximately 15 minutes each. Finally, the cleaned substrates were dried using a nitrogen (N_2) gun before being loaded into the deposition system. Thin films of WS_2 were deposited using RF

*Corresponding author E-mail: aalahmri@kku.edu.sa

magnetron sputtering on soda lime glass substrates. The WS_2 target with a purity of 99.99% and a size of 3 diameters × 3mm thickness was provided by Advanced Engineering Materials (AEM) China.

The sputtering chamber was first purged twice to eliminate any unwanted gases. The turbomolecular pump reduced the chamber pressure to 10^{-6} mbar. At the time of deposition, the operating pressure was kept at 10^{-2} mbar to initiate plasma. The target-to-substrate distance (sputter down) and substrate holder rotation were set to 14 cm and 20 rpm, respectively. Table 1 shows the deposition parameters employed in this study. The substrate temperature was set to 100, 200, 300, and 400 °C during the deposition procedure. To prevent as-grown films from oxidizing, all samples were kept inside the sputtering chamber until preparation was complete and the substrate temperature had returned to room temperature.

Table 1: Sputtering Parameters

Parameter	Condition/Value
Target	WS_2 (99.99% pure)
Substrate	Soda Lime Glass
Base Pressure	4.0×10^{-6} mbar
Working Pressure	1.82×10^{-2} mbar
Growth Temperature	100, 200, 300, and 400 °C
RF Power	150 Watts
Argon Flow Rate	50 sccm

2.2. Characterization

The thickness of the thin films was monitored during deposition using a quartz crystal microbalance (QCM), which is equipped with a sputtering coater. The actual thickness of the prepared thin films was measured with the Alpha-Step IQ Surface Profiler. The structure of the prepared thin films is examined by X-ray Diffraction (XRD) D8 Advance Bruker with a CuKα radiation source with a wavelength of 1.5406 Å. Raman spectra were measured by DXR Raman Microscope (Thermo Scientific Company, USA), with a 532 nm laser as the excitation source. The laser power was set to 2 mW with a 50 µm pinhole aperture. The exposure time for the collection was adjusted to 2 seconds. Measurements of transmittance (T) and reflectance (R) as a function of wavelength were performed using a Cary Series UV–VIS–NIR spectrophotometer at wavelengths ranging from 200 nm to 2500 nm. The surface morphologies of the prepared thin films were examined using a Field Emission Scanning Electron Microscope (JIB-4700F Multi Beam System, Tokyo, Japan). Additionally, atomic force microscopy (AFM) was performed on all prepared films using a Scanning Probe Microscope NT–MDT SOLVER NEXT.

3. Results and Discussion

3.1. XRD and Raman spectroscopy for WS_2 thin films

A comparison of the XRD patterns of WS_2 thin films deposited by RF power at various substrate temperatures is shown in Fig.1. At a substrate temperature equal to room temperature, no distinct peaks corresponding to WS_2 were observed, indicating amorphous or poorly crystalline phases. As the substrate temperature increased from 100 ºC to 400°C, a polycrystalline character of thin films appeared, and the peaks became sharper and more intense, suggesting an improvement in crystallinity. The peaks observed at 2θ values of approximately 14.2°, 33.6°, and 59.5° agree with (002), (100), and (008) planes of hexagonal WS_2 (JCPDS 002-0131). The intensity of the (002) peak increased with temperature, confirming enhanced crystallinity. This suggests improved out-of-plane alignment and reduced defect density.

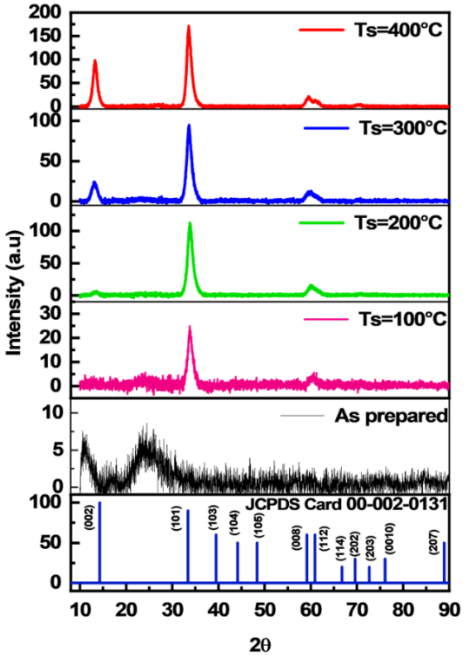

Fig. 1: The XRD chart of WS_2 at different substrate temperatures

The mean crystallite size D was estimated using Scherrer's formula:

$$D = \frac{K\lambda}{\beta \cos\theta} \quad (1)$$

where K is a constant typically known as the crystallite shape parameter. If the exact crystallite shape is unknown, K is typically approximated as 0.9 [6]. The XRD wavelength λ is 1.5406 Å, β (in radians) represents the full width at half-maximum (FWHM) in radians, and θ signifies Bragg's angle. The lattice strain (ε) was determined using the following equation:

$$\varepsilon = \frac{\beta \cot\theta}{4} \quad (2)$$

The dislocation densities (δ) may be determined using the following equation:

$$\delta = \frac{1}{D^2} \quad (3)$$

Crystallites number per unit area N_c , calculated with:

$$N_c = \left[\frac{t}{D^3}\right][unit\ area\ ]^{-1} \quad (4)$$

We calculated the texture coefficient $T_{C(hkl)}$ using the relation [7]:

$$T_{C(hkl)} = \left[\frac{I_{(hkl)}}{I_{0(hkl)}}\right]\left[\frac{1}{N}\sum_N \frac{I_{(hkl)}}{I_{0(hkl)}}\right]^{-1} \quad (5)$$

The details about the crystal structure of all the thin films we made, like crystal size, strain, and dislocation density, are shown in Table 2. The films exhibit improved crystallinity as the substrate temperature rises from 100°C to 400°C. This is indicated by reduced FWHM values and larger crystallite sizes, reflecting more ordered and defect-free growth. Increased atom mobility at higher temperatures is the main cause of the improvement in structural quality. In addition to lowering internal stress and improving layer alignment, this also lowers microstrain and dislocation density. The structural quality reaches its best at 400°C because this temperature produces the largest crystallite size and the lowest defect levels.

Table 2: Crystallite properties of WS_2 at various substrate temperatures.

Substrate temperature (°C)	2θ, (degrees)	FWHM, *b* (degrees)	Crystallite Size, D (nm)	Strain, e×10^{-3}	Dislocation density, d (10^{12} lines/cm^2)	Texture coefficient, $T_{C(101)}$
100	33.82	1.014	8.55	14.56	11.69	1.25
200	33.83	0.919	9.44	13.18	10.59	2.52
300	33.61	0.888	9.76	12.83	10.25	2.18
400	33.58	0.884	9.80	12.78	9.127	1.81

The number of crystallites shows minimal change until 300°C before it experiences a significant increase at 400°C, according to Figure 2. The behavior we observe indicates that grains are beginning to form or that larger nucleation events occur because adatom movement accelerates at higher temperatures.

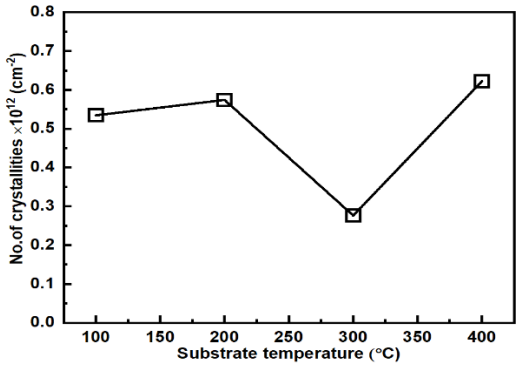

Fig. 2: Number of crystallites at different substrate temperatures.

Crystallite size grows continuously with temperature, while strain decreases steadily, as illustrated in Table 2. Higher temperatures stimulate grain development and reduce internal lattice tension, improving crystallinity and reducing flaws. [8–10]. The (101) plane texture coefficient (T_C) in WS_2 thin films is influenced by substrate temperature, indicating variations in the film-preferred crystal orientation. The low T_C value (1.25) at 100 °C suggests a more random polycrystalline structure due to reduced atomic mobility on the substrate surface. When the temperature reaches 200 °C, the T_C climbs to 2.52, indicating increased atomic mobility and preferential orientation along the (101) plane, making it the ideal temperature for directed development. At 300°C, the T_C decreases to 2.18, possibly due to competing growth directions or strain redistribution in the film. The T_C lowers to 1.81 at 400 °C, indicating a continuous loss in texture (101). Increased thermal energy, atomic desorption, surface roughness, or a change in the growth process could cause this drop. High substrate temperatures impair crystallographic alignment, while moderate temperatures support strong (101) orientation.

The Raman spectra of WS_2 thin films show better crystallinity as the substrate temperature rises from 100°C to 400°C, according to Figure 3.

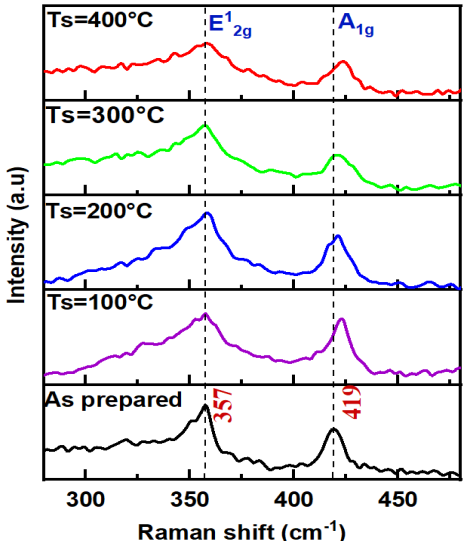

Fig. 3: Micro Raman spectra of WS_2 thin films at varying substrate temperatures.

The Raman spectra, particularly the A_{1g} peaks, exhibit notable shifts in response to changes in substrate temperature, providing insight into the material's structural and electronic characteristics. The temperature-induced Raman frequency shift may result from one of the following factors: thermal expansion of the lattice, anharmonic effects, and strain from the differing thermal expansion coefficients between the substrate and WS_2 [11]. The A_{1g} mode, which corresponds to the motion of two S atoms along the z-axis, is particularly sensitive to thermal expansion and strain, leading to observable shifts in its peak position. As the substrate temperature increases, the A_{1g} peak shows a redshift, indicating a shift to lower wavelengths. The combined effects of thermal expansion and compressive

strain can explain this redshift. Specifically, WS_2 expands more rapidly as the temperature rises than the substrate, resulting in a compressive strain that influences the Raman peak positions [11].

3.2. Morphology of WS_2 thin films

Figure 4 shows the FESEM images of the sputtered WS_2 thin films at different substrate temperatures. All the prepared films showed a tightly woven network of homogeneous and dense microstructure, with no porosity observed. The grown films showed lamellar morphology with nano-wall-like structures. Many researchers also recorded a similar morphology [12-14]. Dense nucleation increased as the substrate temperature rose.

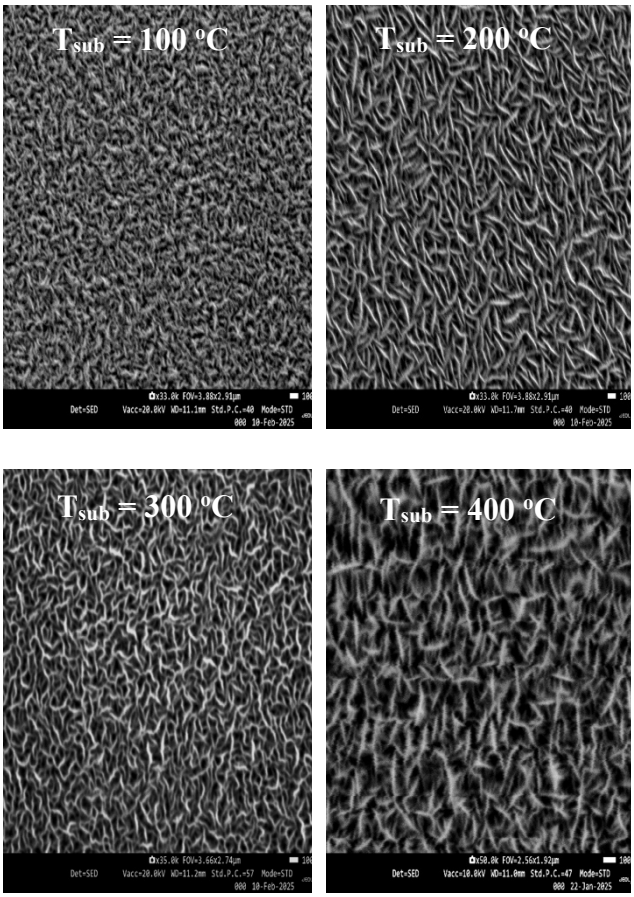

Fig. 4: SEM images of WS_2 thin films grown at different substrate temperatures.

AFM images (5 × 5 µm) of WS_2 films grown on soda lime glass substrates are shown in Fig. 5 (A-D). The AFM images of WS_2 thin films show that the surface morphology improves significantly when the substrate temperature is raised from T_{sub}=100 to 400°C. The films at ambient temperature and 100°C display disordered and flat grains, whereas those at 200°C to 400°C show enhanced grain alignment and crystallinity. The film at 400°C exhibits well-aligned, elongated grains with a uniform distribution, indicating optimal crystalline quality and surface morphology.

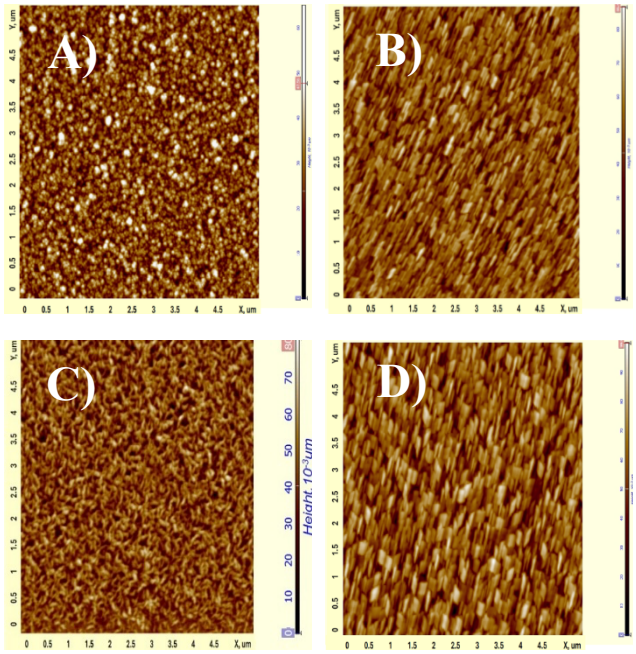

Fig. 5: AFM topographic image (5µm × 5µm) of WS_2 deposited at different substrate temperatures, (A) T_{sub}=100°C, (B) T_{sub}=200°C, (C) T_{sub} = 300°C, and (D) T_{sub}= 400°C.

Table 3: Influence of substrate temperature on surface roughness and grain size of WS_2 thin films

Substrate temperature, °C	Thickness, nm	Roughness root mean square, nm	Roughness average, nm	Grain size, nm
Ts=100°C	334	22.89±2.1	18.76±1.7	59.8±6.7
Ts=200°C	483	18.34±1.4	14.55±1.1	88±8.9
Ts=300°C	257	18.69±1.2	14.26±1.1	97.9±9.6
Ts=400°C	696	16.23±1.4	13.06±1.2	102.6±11.2

As shown in Table 3, the substrate temperature affects the grain size of WS_2 films. Higher temperatures generally result in larger grain sizes due to increased atomic mobility. Moreover, higher temperatures can result in smoother surfaces due to the improved mobility of adatoms on the substrate, allowing for better coalescence and lower roughness [5]. The observed evolution suggests that 400°C represents the optimal temperature for producing WS_2 films with suitable characteristics for electronic or catalytic applications.

3.3. Optical Properties

The substrate temperature during deposition significantly influences the optical characteristics and band gap energy of WS_2 thin films. Understanding these processes is crucial for improving the performance of devices using WS_2, particularly in photovoltaics and electronics. All films showed high optical transmittance (>80%) in the visible spectrum, as shown in Fig. 6-A. The substrate temperature during thin film deposition significantly influences their

structural and optical properties. The films grown at room temperature had no discernible XRD peaks, indicating an absence of periodic structure, which may result in increased reflection, as shown in Fig. 6 - B. The energy band gap of WS_2 is known to change with the number of layers and the structural quality of the films. As the substrate temperature increases, the improved crystallinity may lead to a more direct band gap, which is typically observed in high-quality monolayer WS_2 films [15].

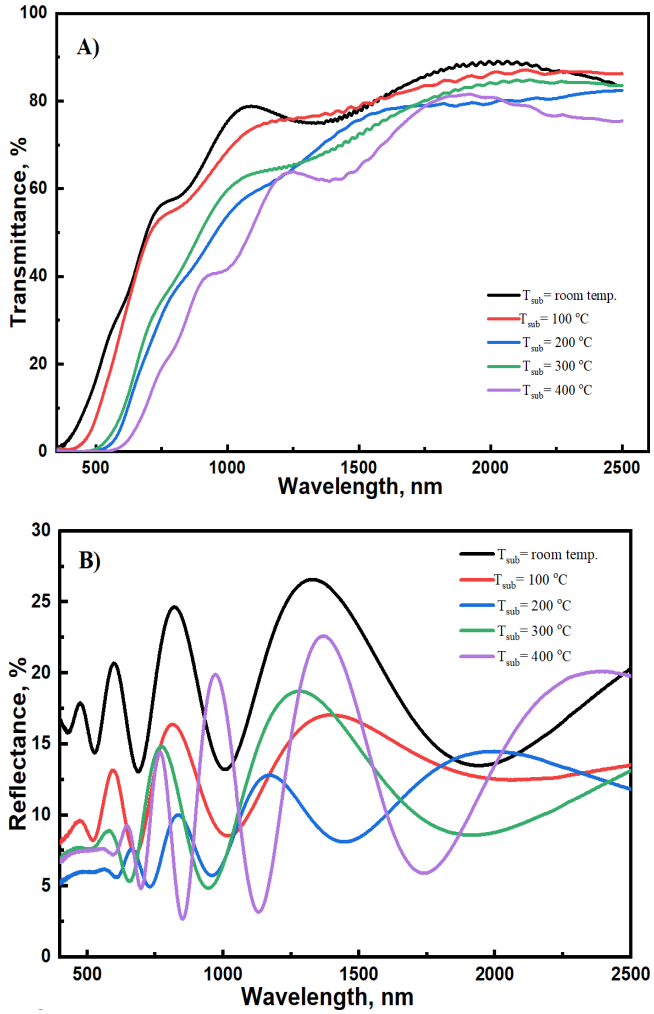

Fig. 6: Transmittance and Reflectance of WS_2 thin films deposited at different substrate temperatures.

The tunable bandgap of WS_2 is a property that is often overlooked despite its importance. The fabrication procedure significantly influences bandgap variability, accommodating various optoelectronic applications [16]. This material can show a wide direct bandgap exceeding 2 eV and a narrower indirect bandgap below 1.5 eV. Furthermore, the structural characteristics of WS_2 are significantly influenced by the relatively large atomic radius of tungsten, which enables the fine-tuning of its properties to meet specific functional needs [16, 17]. To get the absorption coefficient (α) from the transmission and reflection spectrum, use the following equation:

$$\alpha = \frac{1}{d_f}\ln\left\{\frac{(1-R)^2}{2T} + \left[\frac{(1-R)^4}{4T^2} + R^2\right]^{1/2}\right\} \quad (6)$$

To examine whether the optical transition is direct or indirect, we used equation 7 and plotted log $(\alpha h\nu)$ with $\log(h\nu)$ to determine the slope x

$$\alpha h\nu = A(h\nu - Eg)^x \quad (7)$$

where A is a constant, $h\nu$ is the photon energy, E_g is the bandgap, and x is the number that characterizes the transition process. The values of x are 1/2, 3/2, 2, and 3 for direct allowed, direct forbidden, indirect allowed, and indirect forbidden transitions, respectively. The value of x is 0.5, which indicates a direct transition. To evaluate the value of the energy gap, the relation between $(\alpha h\nu)^2$ on the y-axis and $h\nu$ on the x-axis, so the intercept determines the value of the energy gap, as shown in Fig. 7. The energy band gap of WS_2 thin films decreases with increasing substrate temperature, according to Figure 8.

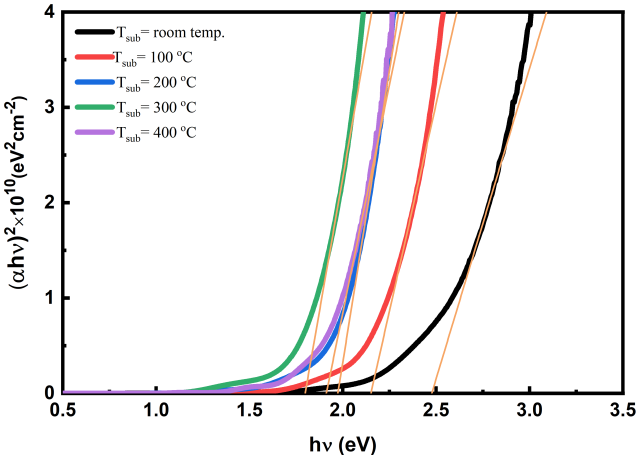

Fig. 7: $(ah\nu)^2$ versus $h\nu$ for WS_2 thin films grown at different substrate temperatures.

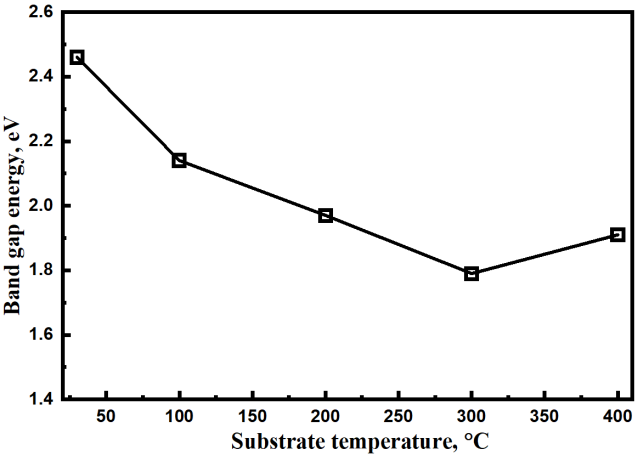

Fig. 8: Band gap energy versus substrate temperatures.

The energy gap of the deposited thin film at room temperature was 2.46 eV, then reduced to 1.79 eV as the substrate temperature increased to 300 °C. The decreased band gap indicates improvements in crystallinity, grain size

growth, and defect or disorder reduction, as indicated in Table 2, all of which reduce the effects of quantum confinement. The minimum band gap at 300°C likely corresponds to optimal film quality, large grains, low strain, and fewer structural imperfections. At 400°C, although the crystallite size increases slightly and structural quality improves, the band gap increases somewhat. This could be suggested due to the re-evaporation of sulfur affecting the stoichiometry of WS_{2-x}. To ensure this, EDX is performed on thin films grown at a substrate temperature of 400 °C, and the result is shown in Figure 9. The elemental composition of the WS_2 thin film is revealed in both weight percent and atomic percent, as illustrated in the inset table. The sample contains 76.99 wt% of tungsten (W) and 23.01 wt% of sulfur (S). The atomic percentages of sulfur and tungsten are 63.15 at% and 36.85 at%, respectively. This stoichiometry indicates a S: W atomic ratio of approximately 1.71:1, slightly lower than the optimal ratio of 2:1 anticipated for stoichiometric WS_2. The sulfur deficiency could arise at T_{sub} = 400 ºC where sulfur atoms, unlike tungsten, sublimate or re-evaporate more easily.

Element	Line	Mass%	Atom%
S	K	23.01±0.15	63.15±0.42
W	M	76.99±0.41	36.85±0.20
Total		100.00	100.00

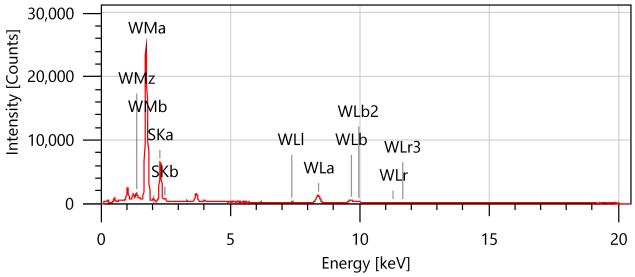

Fig. 9: The Energy Dispersive X-ray Spectroscopy (EDX) analysis of the WS_2 thin film.

A significant deviation from the ideal stoichiometry for WS_2 deposited by sputtering has been reported, with similar findings [5, 13, 15]. In addition, a mismatch between the substrate and WS_2 due to the difference in thermal expansion coefficient leads to thermal stress.

4 Conclusion

This study investigates the impact of substrate temperature on the structural and optical properties of WS_2 thin films created using RF magnetron sputtering. We observed consistent variations in film formation and behavior at temperatures ranging from ambient temperature to 400 °C. Our findings show that substrate temperature significantly impacts the film crystal structure, surface features, and optical properties. XRD and Raman spectroscopy revealed that increasing temperatures improved crystallinity, with the most well-ordered structure observed at 400°C. As the temperature rose, the crystallite size increased while microstrain and dislocation density decreased, indicating stronger, more uniform crystal formation. SEM and AFM images confirmed this, demonstrating that as the temperature increased, the surfaces got smoother and grain sizes increased, both of which are helpful to device performance.

On the optical side, all films showed high transparency within the visible spectrum. As the temperature increased up to 300 °C, the optical band gap reduced, indicating improved crystal quality and fewer structural flaws. However, at 400 °C, the band gap marginally increased again, presumably due to sulfur evaporation at high temperatures. This may lead to a non-stoichiometric WS_{2-x} composition and the development of compressive strain due to the mismatch with the substrate. EDX analysis supported this conclusion and revealed a slight sulfur shortage at 400 °C that sulfurization may treat. These findings indicate that under the deposition conditions with substrate temperatures between 300 and 400°C, WS_2 films have strong structural integrity and desirable optical properties, making them suitable for electronic and optoelectronic applications.

Acknowledgment:

The authors extend their appreciation to the Deanship of Research and Graduate Studies at King Khalid University for funding this work through Large Research Project under grant number (R.G.P.2/472/46).

References

[1] Sikandar Aftab and Hosameldin Helmy Hegazy, Small, 2023, 2205778.

[2] E.C. Serra, V. F. D. Soares, D. A. R. Fernandez, R. Hübler, K. R. C. Juste, C. L. Lima, E. K. Tentardini, Ceramics International, 2019, 45, 19918-19924.

[3] Qing Hua Wang, Kourosh Kalantar-Zadeh, Andras Kis, Jonathan N. Coleman and Michael S. Strano, Nature Nanotechnology, 7, 2012, 699.

[4] Anique Ahmed, Muhammad Zahir Iqbal, Alaa Dahshan, Sikandar Aftab, Hosameldin Helmy Hegazy and El Sayed Yousef, Nanoscale, 16, 2024, 2097.

[5] Md. Khan Sobayel Bin Rafiq, N. Amin, Hamad F. Alharbi, Monis Luqman, Afida Ayob, Yahya S. Alharthi, Nabeel H. Alharthi, Badariah Bais & Md. Akhtaruzzaman, Scientific Reports, 10, 2020, 771.

[6] U. Holzwarth and N. Gibson, Nature Nanotechnology 6, 2011, 534.

[7] M. Jafari, M. M. Shahidi, M. H. Ehsani, Results in Physics 73, 2025, 108232.

[8] W. Ding, D. Han, J. Zhang, and X. Wang, Mater. Res. Express, 6, 2019, 085071.

[9] P. A. Chate, D. J. Sathe, P. P. Hankare, Appl Nanosci, 3, 2013, 19.

[10] P. Sumathi, J. Chandrasekaran, R. Marnadu, S. Muthukrishnan, S. Maruthamuthu, Journal of

Materials Science: Materials in Electronics, 29, 2018, 16815.

[11] Kuilong Li, Wenjia Wang, Journal of Crystal Growth, 540, 2020, 125645.

[12] Bin Rafiq, M.K.S., Amin, N., Alharbi, H.F. et al. WS_2: A New Window Layer Material for Solar Cell Application. Sci Rep 10, 2020, 771.

[13] M. Akhtaruzzaman, M. Shahiduzzaman, N. Amin, G. Muhammad, M. A. Islam, K.S.B. Rafiq, K. Sopian, Nanomaterials, 11, 2021, 1635.

[14] K. Ellmer, phys. stat. sol. (b), 245, 2008,1745.

[15] M. M. S. Villamayor, A. Lindblad, F.O.L. Johansson, T. Tran, N. H. Pham, D. Primetzhofer, N.L.A.N. Sorgenfrei, E. Giangrisotomi, A. Fohlisch, P. Lourenço, R. Bernard, N. Witkowski, G. Pr´evot, T. Nyberg, Vacuum, 188, 2021, 110205.

[16] J. Gusakova, et al., Physica Status Solidi (a) 214(12), 2017, 1700218.

[17] A. Eftekhari, Journal of Materials Chemistry A 5(35), 2017, 18299.